Facile Preparation of Highly Blue Fluorescent Metal Nanoclusters in Organic Media

ARTICLE *in* THE JOURNAL OF PHYSICAL CHEMISTRY C · JANUARY 2011

Impact Factor: 4.77 · DOI: 10.1021/jp209662n

THE JOURNAL OF PHYSICAL CHEMISTRY C

ARTICLE

pubs.acs.org/JPCC

Facile Preparation of Highly Blue Fluorescent Metal Nanoclusters in Organic Media

Xin Huang,[†] Buyi Li,[†] Luo Li,[†] Hui Zhang,[†] Irfan Majeed,[†] Irshad Hussain,[*,‡] and Bien Tan[*,†]

[†]School of Chemistry and Chemical Engineering, Huazhong University of Science and Technology, Wuhan 430074, P. R. China

[‡]Department of Chemistry, LUMS School of Science & Engineering (SSE), D.H.A., Lahore Cantt-54792, Pakistan

Supporting Information

ABSTRACT: A multifunctional polymer ligand, containing thiol, thioether, and ester functional groups, is designed and used to prepare intense blue fluorescent gold nanoclusters (AuNCs) with a diameter of ~1.2 nm and high quantum yield (QY) of 24.3% in organic media without using additional phase-transfer reagents. The size and QY of AuNCs can be fairly controlled by adjusting the molecular weight (M_n) and concentration of multifunctional polymer ligand. The AuNCs retain their fluorescence in various organic solvents and are fairly stable for several months. The same polymer can also be used to prepare silver and platinum nanoclusters (AgNCs and PtNCs), which are not very fluorescent. All of these metal nanoclusters (MNCs) have been characterized thoroughly using TEM, XPS, MALDI-TOF, and other common optical techniques. Apart from the diverse applications of silver and platinum NCs, the highly fluorescent AuNCs may have potential applications in thermal gradient optical imaging, single molecule optoelectronics, sensors and optical components of the detectors.

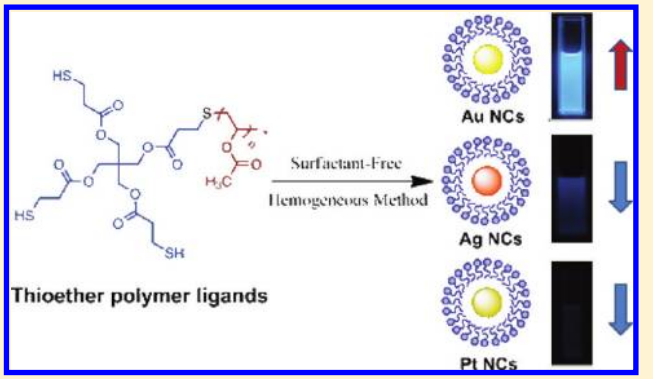

INTRODUCTION

The size and shape of metal particles, especially when below 100 nm, has profound influence on their physical and chemical properties.[1] Bulk metals are known electrical conductors and optical reflectors due to the free movement of electrons in the conduction band.[2] On the contrary, the metal nanoparticles (MNPs), especially those of gold, silver, and copper, exhibit a variety of colors, depending on their size and shape, due to surface plasmon resonance (SPR), which is attributed to the collective oscillation of conduction electrons upon interaction with electromagnetic radiations.[1a,b] The band structure of metals becomes discontinuous and is further broken down to discrete energy levels when the size of their particles is reduced to ~1 nm.[2] These molecule-like metal nanoclusters (MNCs) do not possess any plasmonic behavior but display other interesting optical and catalytic properties.[3] For example, such MNCs, filling the gap between the metal atoms and NPs, can still interact with light via electronic transitions between discrete energy levels resulting in intense light absorption and emission, a phenomenon known as fluorescence.[4] By controlling the number of atoms in MNCs, the gap between the discrete energy levels can be controlled, thus making it possible to control the absorption and emission wavelengths.[5] Because of these size-dependent and unique optical, electrical, and other physical/chemicals properties,[6] the MNCs are now being extensively studied for a host of applications including bioimaging,[7] sensing,[8] optoelectronics,[9] catalysis,[10] and so on.

Keeping in view such attractive applications of MNCs, a considerable interest has recently been witnessed to develop reproducible protocols for the synthesis of MNCs with a fair control over their size, solubility, stability, emission wavelength, and improved quantum yield (QY).[11] The most common protocols in this regard involve either etching of the larger nanoparticles using various thiols,[12] biomolecules,[13] and polymers[14] or controlled reduction of metal ions in the presence of certain capping agents such as glutathione, dendrimers, oligonucleotides, proteins, and so on.[15] Most of these processes are either complicated or produce small amount of nanoclusters along with larger nanoparticles and low QY.[16] Moreover, most of these protocols for MNCs were aimed to produce MNCs in aqueous media for their applications in bioimaging, which usually lead to the formation of red light-emitting nanoclusters.[7d,13a,14c,16d] Photostable and nontoxic blue-light emitting materials are also equally important because of their applications in multicolor displays including electroluminescence devices in addition to bioimaging and so on. The production of such blue light-emitting photostable nanoclusters in organic media offers an additional advantage to produce easily fluorescent thin films of such materials on various surfaces for applications in device fabrication and photocatalysis.

Received: October 8, 2011
Revised: December 8, 2011
Published: December 09, 2011

Herein we report a very simple protocol to prepare size-tunable and highly fluorescent gold nanoclusters (AuNCs) with blue emission by reducing gold precursors in the presence of a multifunctional polymer containing thiol, thioether, and ester functionalities. The size and QY of AuNCs is controllable by controlling the molecular weight and concentration of multifunctional polymers. The homogeneous method employed without any phase transfer reagents (such as cetyltrimethylammonium bromide, tetraoctylammonium bromide, etc.) makes postprocessing steps less complicated and time-consuming, even solving the problem of environmental pollution to some extent. These AuNCs are soluble in a variety of organic solvents, highly stable, and maintain their fluorescence for several months without significant change in emission intensity. More interestingly, the same protocol can also be used to produce silver and platinum nanoclusters (AgNCs and PtNCs), which were not very fluorescent. We believe that these blue-light-emitting AuNCs would be very useful to fabricate optoelectronic devices and as photocatalysts, which can be applied in the field of thermal gradient optical imaging, single molecule optoelectronics, sensors and optical components of the detector, and so on. Moreover, nonfluorescent AgNCs and PtNCs may have interesting applications in catalysis.

EXPERIMENTAL SECTION

Materials. All chemicals were of analytical grade and used as received without any further purification, unless otherwise described. Vinyl acetate ester (VAc, 99.0%), hydrogen tetrachloroaurate ($HAuCl_4 \cdot 4H_2O$, 47.8%), Hexachloroplatinic-(IV) acid hexahydrate ($H_2PtCl_6 \cdot 6H_2O$, 37.0%), silver nitrate ($AgNO_3$, 99.0%), sodium borohydride ($NaBH_4$, 99.0%), 2,2′-azobisisobutyronitrile (AIBN), anhydrous magnesium sulfate ($MgSO_4$), 9,10-diphenylanthracene (99.0%), 2-methyl-9, 10-di(2-naphthyl)anthracene (MADN, 99.0%), *n*-butanol, *n*-hexane, toluene, acetone, anhydrous ethanol, methanol, tetrahydrofuran (THF), and *N*,*N*-dimethylformamide (DMF) were purchased from National Medicines of China. Pentaerythritol tetrakis 3-mercaptopropionate (PTMP, 97.0%) and dodecanethiol (DDT, 99.0%) were obtained from Aldrich.

Synthesis of Thioether Polymer Ligand. In a typical polymer synthesis reaction, 50 mL of methanol solution containing VAc (40.000 g, 0.465 mol), PTMP (11.713 g, 23.250 mmol), and AIBN (1.750 g, 9.300 mmol) were added to a four-necked round-bottomed flask fitted with a reflux condenser under nitrogen with magnetic stirring. The temperature of the reaction mixture was maintained at 62 °C and refluxed for 5 to 6 h. The solvent was removed by rotary evaporator after the reaction. The viscous products were dissolved in THF and then isolated by precipitating into cold *n*-hexane. The excess solvent and monomers were removed by evaporation using a vacuum oven set at 40 °C. A fraction of low molar mass polymer, unreacted monomer, and some oligomers due to incomplete reaction were removed during the precipitation step. The yield of thioether polymer PTMP-PVAc was 26.641 g, 66.6%.

Preparation of MNCs Using PTMP-PVAc. AuNCs and PtNCs were prepared according to the following method. PTMP-PVAc (9 mM) THF solution (5 mL) was added to 15 mL of a 2.0 mM solution of metal salt ($HAuCl_4$ or H_2PtCl_6) in THF under vigorous stirring. After the metal salt/polymer mixture solution was stirred for 0.5 h, freshly prepared $NaBH_4$ solution (2 mL, 6.5 mM) was added to the mixture dropwise. The reaction was then allowed to continue for 5 to 6 h under vigorous stirring. The anhydrous $MgSO_4$ was used to get rid of the water; then, the solution was centrifuged/filtered three times to remove $MgSO_4$. To remove soluble impurities and the excess polymer ligand, we dialyzed the resultant AuNCs and PtNCs in THF solution using dialysis tubing (molecular weight cutoff = 100 000 g/mol) for 24 h. After the dialysis, the solvent was removed from MNCs suspension using a rotary evaporator, and the product was dried at 35 °C for 24 h. Finally, the product was dissolved in 10 mL of THF or other organic solvents such as toluene, chloroform, and DMF.

For AgNCs synthesis, 0.5 mL of a 0.5 mM $AgNO_3$ aqueous solution and 9.5 mL of PTMP-PVAc THF solution were mixed under vigorous stirring. After 0.5 h, freshly prepared $NaBH_4$ solution (5 mL, 0.5 mM) was added dropwise to the mixture. The reaction was then allowed to continue for 5 to 6 h under vigorous stirring. The postsynthetic purification process was the same as that mentioned above for the purification of AuNCs and PtNCs.

Quantum Yield Measurement. The QY of a compound is defined as the fraction of molecules that emit a photon after direct excitation by the source.[17] This quantity is not the same as the total number of emitted photons that escape a bulk sample divided by the total number of absorbed photons, although in many instances the two quantities are nearly equal. The measurement of QY employed the compared method, which is described below (eq 1)

$$\Phi_{unk} = \frac{A_{std}}{A_{unk}} \times \frac{F_{unk}}{F_{std}} \times \frac{{n_{unk}}^2}{{n_{std}}^2} \times \Phi_{std} \quad (1)$$

where Φ is the quantum yield, unk is the unknown sample, std is the standard, n is the refractive index of solvent, A is the absorption at the selected excitation wavelength, and F is the integrated fluorescence signal in the emission region. To calculate the QY of polymer ligand PTMP-PVAc, AuNCs@PTMP-PVAc, AgNCs@PTMP-PVAc, and PtNCs@PTMP-PVAc, we measured a series of the samples and the standard 9,10-diphenylanthracene (Φ = 0.91 in ethanol).[18] All samples were diluted to ensure the optical densities less than 0.02 measured by Lambda 35 UV−visible spectrophotometer (Perkin-Elmer) to reduce the error. The emission spectra were recorded on FP-6500 fluorescence spectrometer (Jasco) under the excitation of 365 nm light.

Transmission Electron Microscopic Analysis of MNCs. The samples for transmission electron microscopy were prepared by slow evaporation of a dilute drop of MNCs on carbon-coated copper grids (400 mesh). Transmission electron micrographs were recorded using a JEOL-2100 electron microscope operating at an acceleration voltage of 200 kV.

Dynamic Light Scattering. The particle's hydrodynamic size was measured by a particle sizer (Zetasizer Nano S) with dynamic light scattering (DLS) and NIBS (Noninvasive Back Scatter) technology from Malvern Instruments (Malvern), which has an effective particle detection capability from 0.6 to 6000 nm. The samples were placed in the quartz cuvette cells and analyzed at 25 °C.

Matrix-Assisted Laser Desorption/Ionization Time-of-Flight. Samples were analyzed using a Bruker Autoflex matrix-assisted laser desorption/ionization time-of-flight (MALDI-TOF)/TOF instrument. Samples (0.5 μL) were spotted on a MALDI target plate with 0.5 μL of CHCA matrix (10 mg/mL CHCA in 50% ACN/0.1%TFA/25 mM diammonium citrate) and externally calibrated with a mixture of angiotensin I (5 pmol/μL), ACTH

Scheme 1. Reaction Scheme for the Synthesis of Thioether Polymer Ligand PTMP-PVAc (a) and Preparation of Fluorescent Au NCs Stabilized by Thioether Polymer Ligand in Homogeneous System (b)

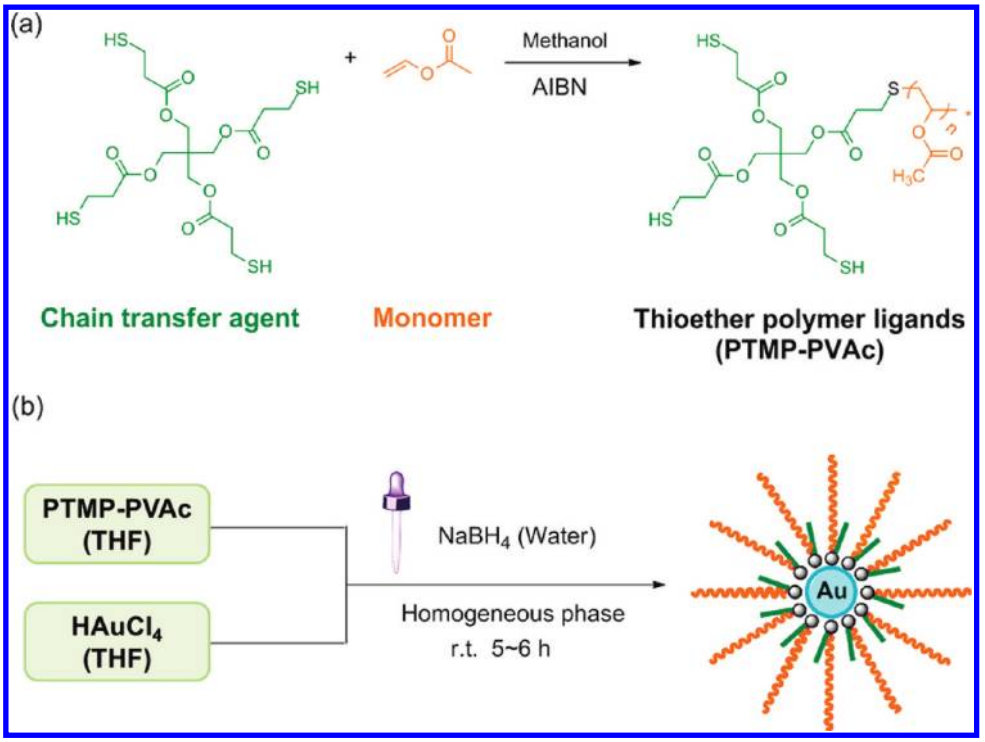

Table 1. PTMP-PVAc Thioether Polymer Ligand with a Range of Molecular Weights

		molecular weight (g/mol)				
item	VAc/thiol (mol/mol)	M_n	M_w	PDI	yield (%)	QY (%)
PTMP-PVAc0.5%	200/1	25 710	47 690	1.855	52.5	4.2
PTMP-PVAc1.0%	100/1	25 570	44 460	1.739	46.3	7.6
PTMP-PVAc2.0%	100/2	19 430	29 980	1.543	72.3	11.7
PTMP-PVAc3.0%	100/3	18 960	28 110	1.483	22.0	11.3
PTMP-PVAc5.0%	100/5	17 180	23 420	1.363	66.6	5.7

(5 pmol/μL), insulin (100 pmol/μL), and cytochrome *c* (100 pmol/μL). The data were processed using FlexAnalysis (Bruker).

X-ray Photoelectron Spectroscopy. The X-ray photoelectron spectroscopy (XPS) spectrum of MNCs was obtained using AXIS-ULTRA DLD high-performance imaging XPS (Shimadzu, Japan). The energy resolution was set to 1.7 eV to minimize data acquisition time, and the photoelectron takeoff angle was 37°.

Fluorescence Spectroscopy. The fluorescence of polymer ligands and MNCs was determined using a FP-6500 fluorescence spectrometer (Jasco) at room temperature using the quartz cuvette cells. The emission spectra were obtained at different excited wavelengths, and the excitation spectra were recorded at the corresponding maximum emission wavelength.

UV−vis Spectrophotometric Analysis. The presence or absence of typical SPR band of metal NPs and metal NCs, respectively, was determined using the Lambda 35 UV−vis spectrophotometer (Perkin-Elmer). For this purpose, the nanoparticle/nanocluster samples were dispersed in toluene, which was also used as a reference solvent.

RESULTS AND DISCUSSION

Synthesis and Characterization of Multifunctional Polymer Ligand. The multifunctional polymer ligands PTMP-PVAc were synthesized by facile chain-transfer radical polymerization method using vinyl acetate ester (VAc) as a monomer, pentaerythritol tetrakis 3-mercaptopropionate (PTMP) as the chain-transfer agent, and methanol as a solvent (Scheme 1a). Through tailoring the amount of chain-transfer agent, a series of different molecular weights (M_n) of PTMP-PVAc was synthesized (Table 1 and Figure S1 of the Supporting Information). The structure of polymer ligands PTMP-PVAc was confirmed by ^{1}H NMR and IR spectroscopy (Figures S2 and S3 of the Supporting Information). Interestingly the multifunctional polymer ligand PTMP-PVAc was found to be fluorescent with an emission peak at 430 nm when excited at 365 nm (Figure S4 of the Supporting Information). However, the solvent, THF, and the chain-transfer agent (PTMP) did not show any emission peak in the region (380−550 nm) when excited at 365 nm. Moreover, the QY of multifunctional ligand was also found to be dependent on its M_n and varied from 4.2 to 11.7%, as shown in Table 1.

dx.doi.org/10.1021/jp209662n |*J. Phys. Chem. C* 2012, 116, 448–455

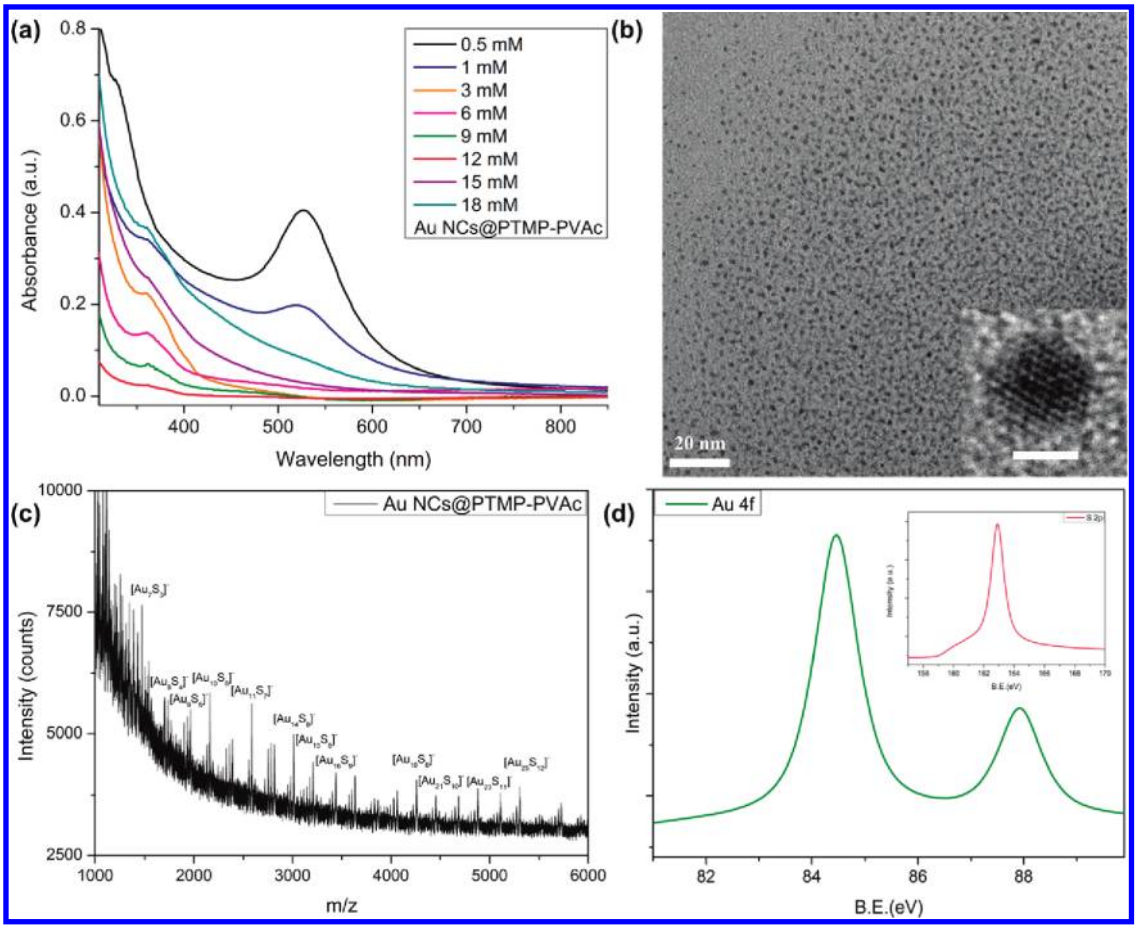

Figure 1. (a) UV−visible absorption spectra of Au NCs@PTMP-PVAc5.0% at different concentrations. (b) Transmission electron micrograph of Au NCs prepared using PTMP-PVAc5.0% at the concentration of 9 mM. Insert graph is the HR-TEM of Au NCs. (c) XPS spectrum of Au NCs@PTMP-PVAc5.0% (9 mM). (d) MALDI-TOF MS of Au_7 in the negative mode showing the presence of Au_7S_3.

Synthesis and Characterization of AuNCs. AuNCs were prepared using the aforementioned multifunctional polymer ligand PTMP-PVAc of different M_n as a capping agent in organic media (THF) without using any additional phase transfer reagent (Scheme 1b). TGA profile (Figure S5 of the Supporting Information) shows weight loss at two different temperatures, similarly to what already was observed with PTMP-PVAc. The Au content of the samples, determined by TGA analysis, was found to amount to 4%. It is known that optical properties (absorption and fluorescence) of MNPs/nanoclusters are highly dependent on their size, in addition to various other factors. The size of fluorescent MNCs is also the key factor to influence the QY of fluorescent nanoparticles.[19] By tailoring the M_n and concentration of polymer, we were able to produce a series of AuNCs with different sizes. The diameter of AuNPs/AuNCs varied from 1.2 to 6.2 nm depending on the M_n of polymer ligand at a constant concentration of 9 mM (Figure S6 of the Supporting Information). A slight increase in the particle size was observed by increasing the M_n of polymer ligands, which is consistent with our previous report.[19] It may be due to the fact that high-molecular-weight polymers take more time to approach and passivate growing metal nuclei due to their slow rate of diffusion. It is worth noticing that although the QY of PTMP-PVAc2.0% polymer was the highest (11.7%), the diameter of Au NPs@PTMP-PVAc2.0% was found to be 3.2 nm and was thus not much fluorescent. PTMP-PVAc5.0%, however, yielded

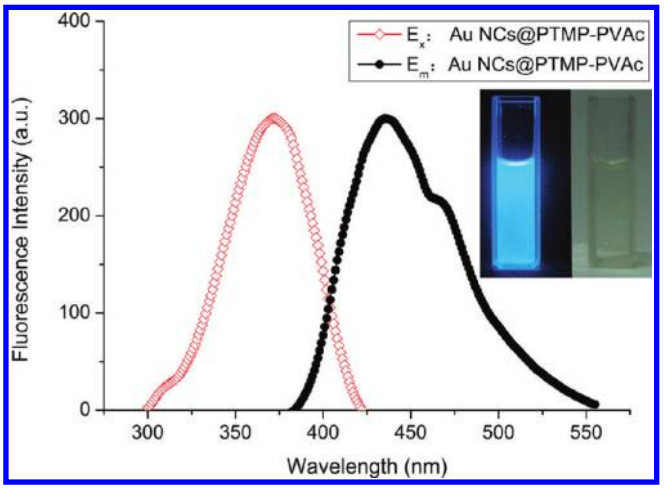

Figure 2. Fluorescence excitation and emission spectra of Au NCs prepared by polymer ligand PTMP-PVAc5.0% with the concentration at 9 mM. Insert is the photograph of the Au NCs@PTMP-PVAc5.0% (9 mM, left) and solvent THF (right) under UV light.

smaller AuNCs (~1.2 nm), which were highly fluorescent. The concentration of polymer is another important factor that affects the size of MNPs. Therefore, to examine the effect of concentration of multifunctional polymer ligand, we prepared a series of

dx.doi.org/10.1021/jp209662n |J. Phys. Chem. C 2012, 116, 448–455

AuNPs using different concentration of PTMP-PVAc5.0%. Lower concentration of polymer ligand (0.5 and 1 mM) resulted in the formation of larger AuNPs (4.0 and 3.6 nm, respectively), which showed a surface plasmon resonance absorption peak at ~520 nm (Figure 1a). Increasing the concentration of polymer to 9, 12, and 15 mM, however, resulted in the formation of smaller AuNCs (<2 nm) with no SPR absorption band, which also correspond to the DLS results (Figure S7 of the Supporting Information). Surprisingly, the diameter of AuNPs increased as we further increased the concentration of polymer ligand beyond 15 mM. For example, 2.5 nm Au NPs were formed using 18 mM polymer ligand. The size of AuNCs obtained using 9−15 mM of polymer ligand varied from 1.1 to 1.3 nm. Transmission electron microscopic analysis (Figure 1b) of AuNCs@PTMPPVAc5.0% (9 mM) confirmed the formation of ~1.2 ± 0.9 nm AuNCs, which is also consistent with DLS results. To find the nature of the core of AuNCs, mass spectrometric analysis was carried out using MALDI-TOF mass spectrometry. The spectrum was collected in the negative mode using a cyano-4-hydroxycinnamic acid (CHCA) as the matrix. The mass spectrum (Figure 1c) is composed of several groups of peaks with spacing of m/z 197 or 229 between the major peaks, which correspond to the loss of Au or AuS. The m/z spacing between isolated peaks in each cluster of peaks is 32 on account of sulfur, and each bunch of peaks can be assigned as $[Au_mS_n]^-$. The m/z of the highest peak is 1476, which indicates that the structure of AuNCs is $[Au_7S_3]^-$ with seven core gold atoms. XPS analysis was also carried out to identify the structure of AuNCs. The results (Figure 1d) show that the $4f_{7/2}$ and $4f_{5/2}$ BEs of Au are 84.2 and 87.9 eV, respectively, and the 2p BEs of S are 162.8 eV, which is a bit higher than that of the typical thiolates (162.0 eV). From the XPS data, the Au/S atomic ratio is 2.31, which is inconsistent with a composition of $[Au_7S_3]^-$. (The expected value is 2.33.)

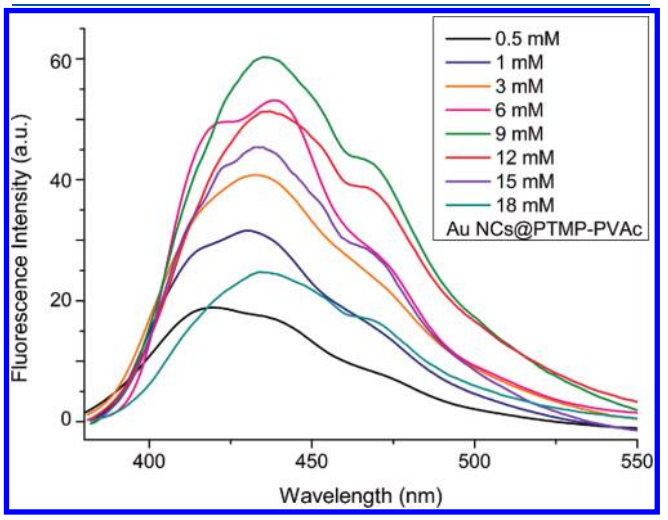

Figure 3. Fluorescence emission spectra of Au NCs@PTMP-PVAc5.0% at different concentrations.

AuNCs were also characterized using fluorescence spectroscopy. When AuNCs@PTMP-PVAc5.0% (9 mM) were excited at 365 nm, they showed a clear emission peak at 435 nm, as shown in Figure 2. The inset of Figure 2 shows the optical micrograph of these AuNCs showing intense blue fluorescence under UV light. The change in the concentration of multifunctional polymer (PTMP-PVAc5.0%) has little effect on the position of the emission peaks of resulting AuNCs. A slight red shift in the emission wavelength was observed by increasing the concentration of polymer from 0.5 to 18 mM (Figure 3). For example, at a polymer concentration of 0.5 mM, the emission wavelength is 421 nm, which is red-shifted to 435 and 436 nm when the concentration of polymer is increased from 9 to 18 mM, respectively. Furthermore, it is worth noticing that a new emission peak near 460 nm appeared when the concentration of polymer was increased beyond 9 mM.

The QY of AuNCs@PTMP-PVAc5.0% was determined using 9,10-diphenylanthracene as a standard, and the results are summarized in Figure 4. Among all samples, Au NCs formed by PTMP-PMAA5.0% at a concentration of 9 mM possess the highest QY, that is, 24.3%. This higher QY of AuNCs could be due to an increase in the positivity of metal core due to the close proximity of several electron withdrawing atoms (O atoms in this case), as has recently been elegantly demonstrated by Jin et al.[20] The QY of AuNCs/AuNPs, however, decreased significantly with a decrease in the concentration of polymer due to an increase in the size of AuNCs, ultimately leading to the formation of AuNPs. For example, using the polymer ligand PTMP-PVAc5.0%, the QY of AuNCs/AuNPs was found to be 4.1, 3.8, and 1.7% as the concentration of polymer was reduced to 3, 1, and 0.5 mM, respectively. In fact, at a polymer concentration of below 6 mM, no AuNCs are formed but the AuNPs that possess a characteristic plasmon resonance absorption band but are not

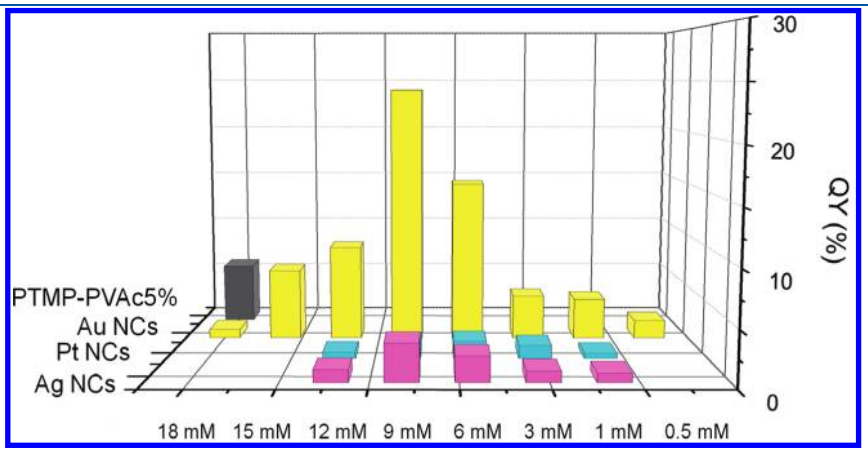

Figure 4. Histogram of the influence of polymer concentration on the quantum yield of Au NCs, Ag NCs, Pt NCs, and polymer ligand PTMP-PVAc5.0%. The used polymer concentrations are 0.5, 1, 3, 6, 9, 12, 15, and 18 mM, respectively.

fluorescent. These AuNPs have also the ability to quench the fluorescence due to polymer itself. However, as the concentration of polymer increases to 6, 9, 12, and 15 mM, it leads to the formation of AuNCs with the QY of 15.1, 24.3, 8.9, and 6.6%, respectively. The fluorescence of these molecule-like AuNCs is probably originated from a LUMO−HOMO transition that can be called an intraband (sp-sp) transition. Additionally, the interaction of polymer ligand with several electron-withdrawing groups with core of Au NCs could also contribute to the increase in fluorescence.[20]

Synthesis and Characterization of AgNCs and PtNCs. Interestingly, the multifunctional polymer (PTMP-PVAc5.0%) can also be used to prepare Ag and Pt nanoclusters/nanoparticles (NCs/NPs), thus demonstrating their wider scope for the preparation of a range of MNCs/NPs without any additional phase transfer reagents in organic media. Importantly, the size of AgNCs/AgNPs and PtNCs/PtNPs can also be fairly controlled by adjusting the concentration of polymer. In the case of Ag NCs/Ag NPs, their size can be controlled between 0.2 and ∼7.3 nm simply by varying the concentration of polymer from 1 to 12 mM, as evident from DLS spectra of these NCs/NPs (Figure S8 of the Supporting Information). Similarly, the size of PtNCs/PtNPs varies from ∼7 to 1 nm as we increase the concentration of polymer from 1 to 12 mM, which is also evident from DLS spectra of PtNCs/PtNPs (Figure S9 of the Supporting Information). In the case of Ag NPs, which are formed when the concentration of polymer is <6 mM, a characteristic damped surface plasmon absorption band is noticed (Figure S10 of the Supporting Information) between 300 and 500 nm while using 1 and 3 mM polymer solution. By increasing the concentration of polymer beyond 6 mM, no such absorption band is present, which indicates the formation of smaller AgNCs (Figure S10 of the Supporting Information). These observations are also supported by DLS data of these AgNCs/AgNPs. Among these samples, with the concentration of polymer set at 9 mM for both AgNCs/AgNPs and PtNCs/PtNPs the diameters of NCs are the smallest, 2.1 ± 1.2 and 1.7 ± 1.1 nm, respectively (Figure 5). XPS results exhibit the information of the photoelectron spectrum of Ag NCs in the 3d region. The $3d_{5/2}$ and $3d_{3/2}$ BEs of

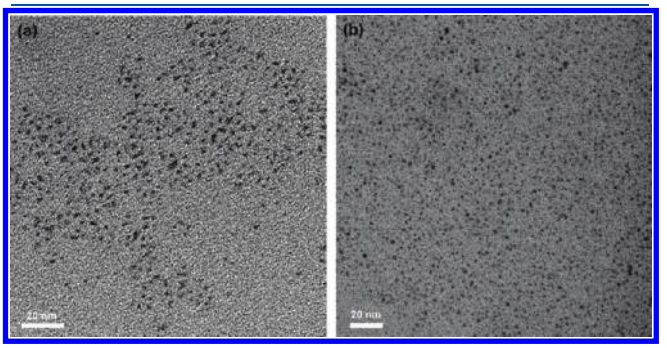

Figure 5. TEM graph of Pt NCs stabilized with polymer ligands PTMP-PVAc (a) and Ag NCs stabilized with polymer ligands PTMP-PVAc (b).

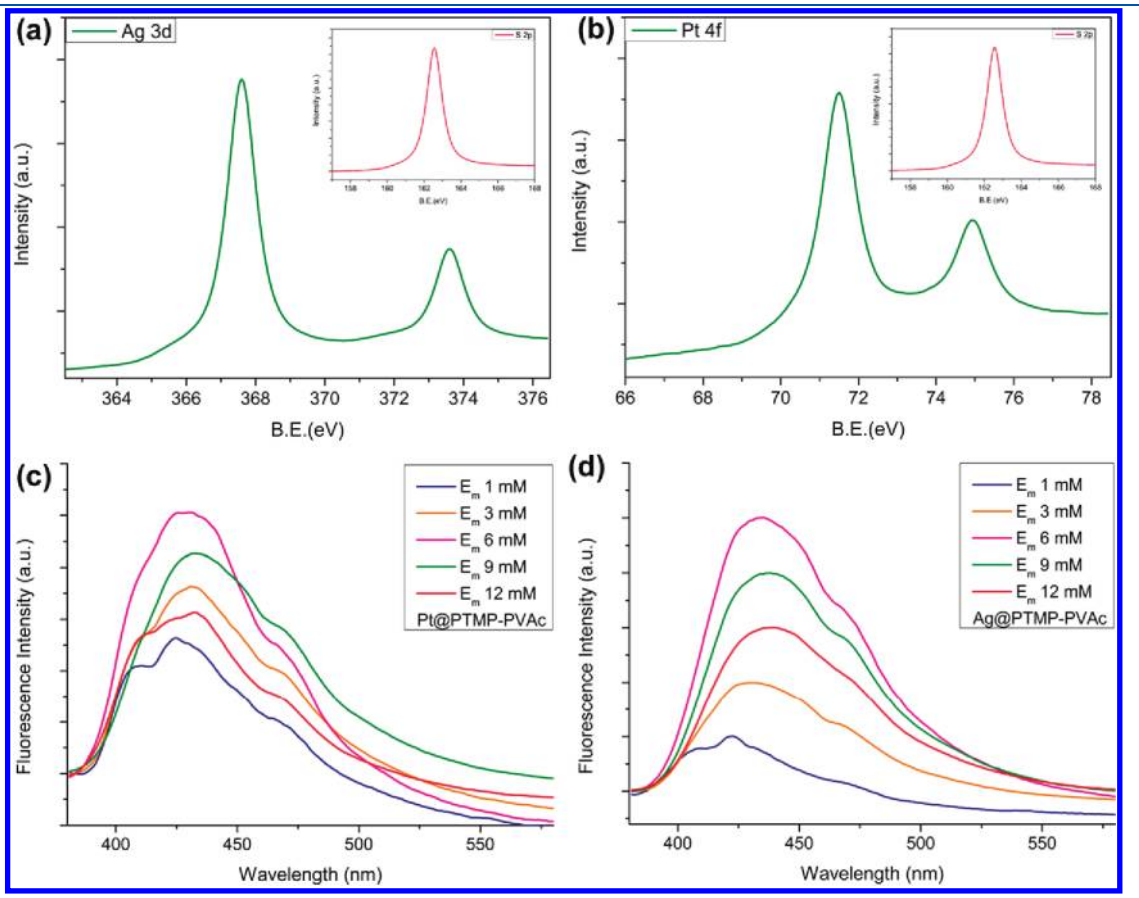

Figure 6. (a) XPS spectra of Ag NCs@PTMP-PVAc5.0% (9 mM). (b) XPS spectra of Pt NCs@PTMP-PVAc5.0% (9 mM). (c) Fluorescence emission spectra of Ag NCs@PTMP-PVAc5.0% at different concentrations. (d) Fluorescence emission spectra of Pt NCs@PTMP-PVAc5.0% at different concentrations.

dx.doi.org/10.1021/jp209662n |J. Phys. Chem. C 2012, 116, 448–455

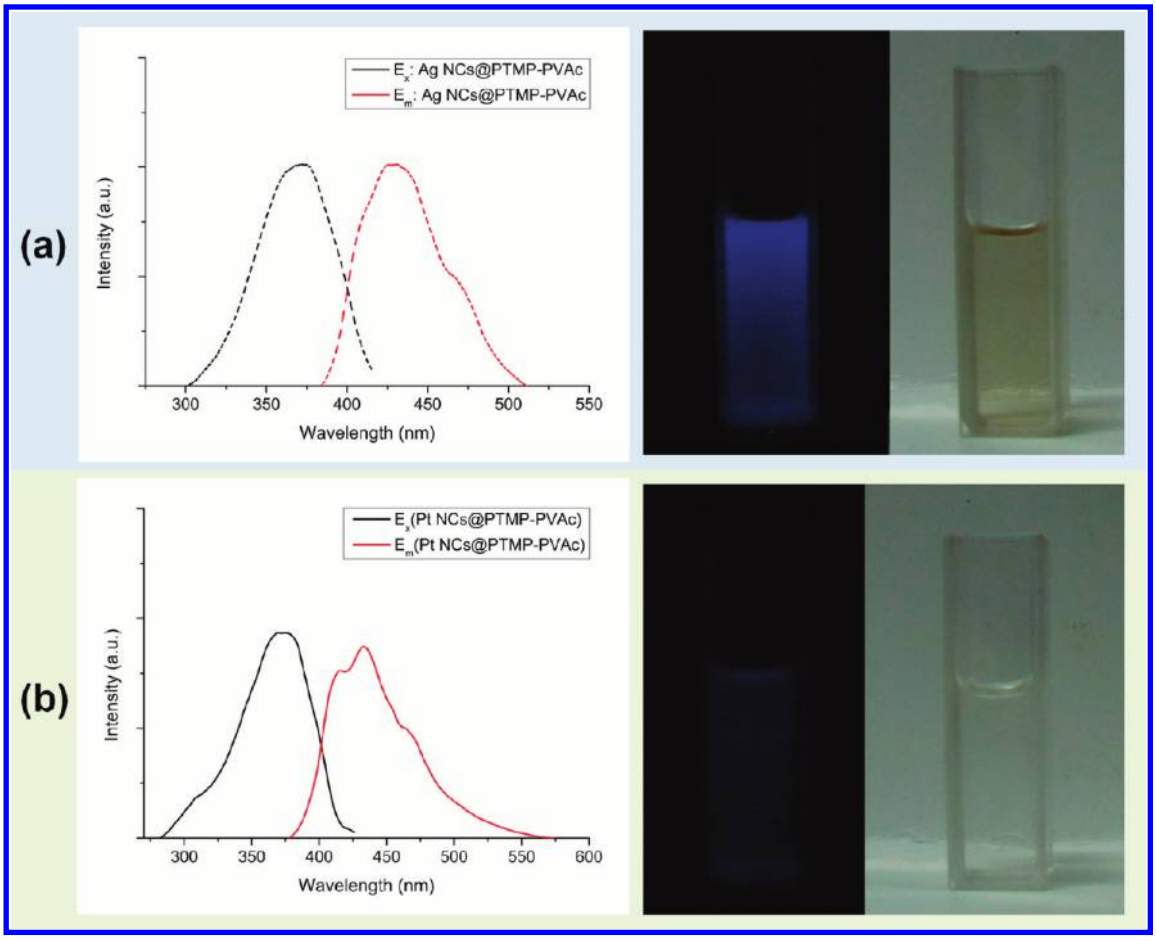

Figure 7. Fluorescence excitation and emission spectra of Ag NCs (a) and Pt NCs (b) prepared by PTMP-PVAc5.0% with the concentration at 9 mM. The corresponding photographs are recorded under the irradiation of day light (left) and 365 nm ultraviolet light (right).

silver are 367.6 and 373.6 eV, respectively (Figure 6a). Similarly, the XPS spectrum of Pt NCs in the 4f region shows that the $4f_{7/2}$ and $4f_{5/2}$ BEs of platinum are 71.6 and 74.9 eV, respectively (Figure 6b). Unlike the AuNCs and AgNCs, PtNCs do not possess any surface plasmon resonance absorption band in the visible region (Figure S11 of the Supporting Information). None of the PtNCs and AgNCs showed any significant emission when excited at 365 nm but only weak emission (Figure 6c,d respectively). The highest QYs of the AgNCs and PtNCs samples were found to be only 3.0 and 1.6%, respectively (Figure 7). In these cases, the emission spectrum was also blue-shifted to 432 and 427 nm, respectively, compared with the emission of AuNCs at 435 nm. We are now trying to improve the QY of PtNCs and AgNCs and further understand the mechanism of formation of MNCs by examining the effect of the structure and M_n of polymer ligands and other reaction conditions for the formation of size-controlled Ag and PtNCs.

CONCLUSIONS

A facile and simple preparation of highly blue fluorescent Au NCs soluble in a variety of organic solvents is reported using a multifunctional polymer ligand PTMP-PVAc without using any additional phase transfer reagents. The size and QY of these AuNCs is controllable by adjusting the concentration and molecular weight of the polymer. The maximum QY of AuNCs was found to be 24.3%, which is probably due to the presence of highly electronegative atoms in the close vicinity of AuNCs. These AuNCs are fairly stable over a period of several months and retain their fluorescence in a variety of organic solvents. The same approach can also be used to prepare size-controlled Ag and Pt nanoclusters/nanoparticles, which are less fluorescent. Apart from the applications of AgNCs/Ag NPs and PtNCs/PtNPs, oil-soluble AuNCs may have potential applications in thermal gradient optical imaging, single molecule optoelectronics, sensors and optical components of the detector, and so on.

ASSOCIATED CONTENT

Supporting Information. Some details of thioether polymer ligands characterization: gel permeation chromatography, ^{1}H NMR spectroscopy, fluorescence spectroscopy, and thermogravimetric analysis. The characterization of AuNCs@PTMP-PVAc, AgNCs@PTMP-PVAc, and PtNCs@PTMP-PVAc: infrared spectroscopy, thermogravimetric analysis, DLS spectra, and UV−visible absorption spectra. This material is available free of charge via the Internet at http://pubs.acs.org.

AUTHOR INFORMATION

Corresponding Author

*Fax: +86 27 87543632; Tel: +86 27 87558172; E-mail: bien.tan@mail.hust.edu.cn. (B.T.). Fax: +92 42 35608314; Tel: +92 42 3560 8133; Email: ihussain@lums.edu.pk (I. H.).

■ ACKNOWLEDGMENT

We thank National Natural Science Foundation of China (50973037, 51173058) for financial support and Huazhong University of Science & Technology Analytical and Testing Center for characterization assistance. We thank Professor Francesco Stellacci at EPFL, Switzerland, for useful discussion. I.H. also thanks LUMS for the start-up grant to initiate nanomaterials research at SSE.

■ REFERENCES

(1) (a) El-Sayed, M. A. *Acc. Chem. Res.* **2001**, *34*, 257–264. (b) Eustis, S.; El-Sayed, M. A. *Chem. Soc. Rev.* **2006**, *35*, 209–217. (c) Love, J. C.; Estroff, L. A.; Kriebel, J. K.; Nuzzo, R. G.; Whitesides, G. M. *Chem. Rev.* **2005**, *105*, 1103–1170.

(2) Diez, I.; Ras, R. H. A. *Nanoscale* **2011**, *3*, 1963–1970.

(3) (a) Wittmann, S.; Schatz, A.; Grass, R. N.; Stark, W. J.; Reiser, O. *Angew. Chem., Int. Ed.* **2010**, *49*, 1867–1870. (b) Friedrich, H.; de Jongh, P. E.; Verkleij, A. J.; de Jong, K. P. *Chem. Rev.* **2009**, *109*, 1613–1629. (c) Tsunoyama, H.; Ichikuni, N.; Sakurai, H.; Tsukuda, T. *J. Am. Chem. Soc.* **2009**, *131*, 7086–7093. (d) Ray, P. C. *Chem. Rev.* **2010**, *110*, 5332–5365. (e) Bakr, O. M.; Amendola, V.; Aikens, C. M.; Wenseleers, W.; Li, R.; Dal Negro, L.; Schatz, G. C.; Stellacci, F. *Angew. Chem., Int. Ed.* **2009**, *48*, 5921–5926.

(4) Diez, I.; Jiang, H.; Ras, R. H. A. *Chem. Phys. Chem.* **2010**, *11*, 3100–3104.

(5) Diez, I.; Pusa, M.; Kulmala, S.; Jiang, H.; Walther, A.; Goldmann, A. S.; Muller, A. H. E.; Ikkala, O.; Ras, R. H. A. *Angew. Chem., Int. Ed.* **2009**, *48*, 2122–2125.

(6) (a) Chen, S.; Ingram, R. S.; Hostetler, M. J.; Pietron, J. J.; Murray, R. W.; Schaaff, T. G.; Khoury, J. T.; Alvarez, M. M.; Whetten, R. L. *Science* **1998**, *280*, 2098–2101. (b) Xiao, L.; Tollberg, B.; Hu, X. K.; Wang, L. C. *J. Chem. Phys.* **2006**, *124*, 114309. (c) Ferreira, H. S.; Rangel, M. D. *Quim. Nova* **2009**, *32*, 1860–1870. (d) Yuan, C. T.; Chou, W. C.; Tang, J.; Lin, C. A.; Chang, W. H.; Shen, J. L.; Chuu, D. S. *Opt. Express* **2009**, *17*, 16111–16118. (e) Muhammed, M. A. H.; Pradeep, T. *J. Cluster Sci.* **2009**, *20*, 365–373.

(7) (a) Boyer, D.; Tamarat, P.; Maali, A.; Lounis, B.; Orrit, M. *Science* **2002**, *297*, 1160–1163. (b) Weissleder, R. *Science* **2006**, *312*, 1168–1171. (c) Lin, C.-A. J.; Yang, T.-Y.; Lee, C.-H.; Huang, S. H.; Sperling, R. A.; Zanella, M.; Li, J. K.; Shen, J.-L.; Wang, H.-H.; Yeh, H.-I.; Parak, W. J.; Chang, W. H. *ACS Nano* **2009**, *3*, 395–401. (d) Wu, X.; Ming, T.; Wang, X.; Wang, P.; Wang, J.; Chen, J. *ACS Nano* **2009**, *4*, 113–120.

(8) Abdiaziz, A. F.; Juan, P. B.-V.; Ramon, A. A.-P.; Jae-Young, C.; Hicham, F. *Small* **2009**, *5*, 1283–1286.

(9) (a) Lee, T.-H.; Gonzalez, J. I.; Zheng, J.; Dickson, R. M. *Acc. Chem. Res.* **2004**, *38*, 534–541. (b) Homberger, M.; Simon, U. *Philos. Trans. R. Soc., A* **2010**, *368*, 1405–1453.

(10) (a) Landon, P.; Collier, P. J.; Papworth, A. J.; Kiely, C. J.; Hutchings, G. J. *Chem. Commun.* **2002**, 2058–2059. (b) Friedrich, H.; de Jongh, P. E.; Verkleij, A. J.; de Jong, K. P. *Chem. Rev.* **2009**, *109*, 1613–1629. (c) Schätz, A.; Reiser, O.; Stark, W. J. *Chem.—Eur. J.* **2010**, *16*, 8950–8967.

(11) (a) Kawasaki, H.; Yamamoto, H.; Fujimori, H.; Arakawa, R.; Inada, M.; Iwasaki, Y. *Chem. Commun.* **2010**, *46*, 3759–3761. (b) Bao, Y. P.; Yeh, H. C.; Zhong, C.; Ivanov, S. A.; Sharma, J. K.; Neidig, M. L.; Vu, D. M.; Shreve, A. P.; Dyer, R. B.; Werner, J. H.; Martinez, J. S. *J. Phys. Chem. C* **2010**, *114*, 15879–15882. (c) Yabu, H. *Chem. Commun.* **2011**, *47*, 1196–1197. (d) Fang, Y. M.; Song, J.; Li, J. A.; Wang, Y. W.; Yang, H. H.; Sun, J. J.; Chen, G. N. *Chem. Commun.* **2011**, *47*, 2369–2371.

(12) (a) Wu, Z. W.; Gayathri, C.; Gil, R. R.; Jin, R. C. *J. Am. Chem. Soc.* **2009**, *131*, 6535–6542. (b) Rao, T. U. B.; Pradeep, T. *Angew. Chem., Int. Ed.* **2010**, *49*, 3925–3929. (c) Jin, R. C. *Nanoscale* **2010**, *2*, 343–362.

(13) (a) Xie, J. P.; Zheng, Y. G.; Ying, J. Y. *J. Am. Chem. Soc.* **2009**, *131*, 888–889. (b) Tanaka, S. I.; Miyazaki, J.; Tiwari, D. K.; Jin, T.; Inouye, Y. *Angew. Chem., Int. Ed.* **2011**, *50*, 431–435. (c) Lan, G. Y.; Chen, W. Y.; Chang, H. T. *Biosens. Bioelectron.* **2011**, *26*, 2431–2435. (d) Wen, F.; Dong, Y. H.; Feng, L.; Wang, S.; Zhang, S. C.; Zhang, X. R. *Anal. Chem.* **2011**, *83*, 1193–1196. (e) Le Guevel, X.; Daum, N.; Schneider, M. *Nanotechnology* **2011**, *22*, 275103.

(14) (a) Zhang, J. G.; Xu, S. Q.; Kumacheva, E. *Adv. Mater.* **2005**, *17*, 2336–2340. (b) Duan, H. W.; Nie, S. M. *J. Am. Chem. Soc.* **2007**, *129*, 2412–2415. (c) Schaeffer, N.; Tan, B.; Dickinson, C.; Rosseinsky, M. J.; Laromaine, A.; McComb, D. W.; Stevens, M. M.; Wang, Y. Q.; Petit, L.; Barentin, C.; Spiller, D. G.; Cooper, A. I.; Lévy, R. *Chem. Commun.* **2008**, 3986–3988. (d) Shang, L.; Dong, S. J. *Chem. Commun.* **2008**, 1088–1090.

(15) (a) Zheng, J.; Petty, J. T.; Dickson, R. M. *J. Am. Chem. Soc.* **2003**, *125*, 7780–7781. (b) Zheng, J.; Zhang, C.; Dickson, R. M. *Phys. Rev. Lett.* **2004**, *93*, 077402–4. (c) Shi, X. Y.; Ganser, T. R.; Sun, K.; Balogh, L. P.; Baker, J. R. *Nanotechnology* **2006**, *17*, 1072–1078. (d) Triulzi, R. C.; Micic, M.; Giordani, S.; Serry, M.; Chiou, W. A.; Leblanc, R. M. *Chem. Commun.* **2006**, 5068–5070. (e) Zheng, J.; Nicovich, P. R.; Dickson, R. M. *Annu. Rev. Phys. Chem.* **2007**, *58*, 409–431. (f) Adhikari, B.; Banerjee, A. *Chem. Mater.* **2010**, *22*, 4364–4371. (g) Adhikari, B.; Banerjee, A. *Chem.—Eur. J.* **2010**, *16*, 13698–13705.

(16) (a) Wilcoxon, J. P.; Martin, J. E.; Parsapour, F.; Wiedenman, B.; Kelley, D. F. *J. Chem. Phys. B* **1998**, *108*, 9137–9143. (b) Bigioni, T. P.; Whetten, R. L.; Dag, O. *J. Phys. Chem. B* **2000**, *104*, 6983–6986. (c) Wang, Z. J.; Cai, W.; Sui, J. H. *Chem. Phys. Chem.* **2009**, *10*, 2012–2015. (d) Muhammed, M. A. H.; Verma, P. K.; Pal, S. K.; Kumar, R. C. A.; Paul, S.; Omkumar, R. V.; Pradeep, T. *Chem.—Eur. J* **2009**, *15*, 10110–10120.

(17) Crosby, G. A.; Demas, J. N. *J. Phys. Chem. A* **1971**, *75*, 991–1024.

(18) Mardelli, M.; Olmsted, J. *J. Photochem.* **1977**, *7*, 277–285.

(19) (a) Huang, X.; Li, B.; Zhang, H.; Hussain, I.; Liang, L.; Tan, B. *Nanoscale* **2011**, *3*, 1600–1607. (b) Huang, X.; Luo, Y.; Li, Z.; Zhang, H.; Li, B.; Irfan, M.; Zou, P; Tan, B. *J. Phys. Chem. C* **2011**, *115*, 16753–16763. (c) Zhang, H.; Huang, X.; Li, L.; Zhang, G. *Chem. Commun.* **2012**, *48*, 567–569. (d) Huang, X.; Zhang, H.; Liang, L. Y.; Tan, B. E. *Prog. Chem.* **2010**, *22*, 953–961.

(20) Wu, Z.; Jin, R. *Nano Lett.* **2010**, *10*, 2568–2573.